Power Independent of Number of Slices (PINS) Radiofrequency Pulses for Low-Power Simultaneous Multislice Excitation

David G. Norris,[1–3]* Peter J. Koopmans,[1,2] Rasim Boyacioğlu,[1] and Markus Barth[1,2]

This communication describes radiofrequency pulses capable of performing spatially periodic excitation, inversion, and refocusing. The generation of such pulses either by multiplication of existing radiofrequency pulses by a Dirac comb function or by means of Fourier series expansion is described. Practical schemes for the implementation of such pulses are given, and strategies for optimizing the pulse profile at fixed pulse duration are outlined. The pulses are implemented using a spin-echo sequence. The power deposition is independent of the number of slices acquired, and hence the power deposition per slice is considerably reduced compared to multislice imaging. Excellent image quality is obtained both in phantoms and in images of the human head. These pulses should find widespread application for multiplexed imaging, in particular at high static magnetic field strengths and for pulse sequences that have a high radiofrequency power deposition and could lead to dramatic increases in scanning efficiency. Magn Reson Med 66:1234–1240, 2011. © 2011 Wiley Periodicals, Inc.

Key words: radiofrequency pulses; multiplexed imaging; radiofrequency power deposition

The simultaneous excitation of multiple slices was originally used in MR in the context of Hadamard encoding (1). Subsequently, a separate phase modulation of each slice was used to stack the slice images along the phase-encoding direction (2). With the advent of techniques for partial parallel imaging (3–5), it became possible to distinguish the signal from simultaneously excited slices on the basis of differences in the sensitivity profiles of the receiver coils. The original demonstration of this technique (6) used SENSE reconstruction (4). This study was long neglected but in the recent past has received increased attention as a method for increasing the speed of echo-planar imaging acquisitions (7,8).

Hitherto, the standard method for generating radiofrequency (RF) pulses for simultaneous excitation has been to sum a set of RF pulses, each of which excited a single slice, with an offset determined by the phase gradient of the pulse. This method can successfully excite a limited number of slices with an excitation profile corresponding to that of the individual RF pulses. Such pulses can easily exceed the specific absorption rate (SAR) limits even for relatively modest combinations of the number of slices and the pulse angle.

Cardiac tagging has long been achieved using pulses with a far lower power deposition (9–11), based on those used for solvent suppression in high-resolution NMR (11). More recently, cardiac tagging has been achieved using a sinc-modulated RF pulse train (12). These pulse forms are exclusively used for the saturation of magnetization. In the context of velocity-selective excitation (13), both refocused excitation and inversion pulses have been proposed and demonstrated (14).

The purpose of this communication is to demonstrate how such RF pulses can be used for imaging purposes. Instead of leading to an increase in RF power deposition, these pulses have a comparable power deposition to that of a pulse required to excite a single slice, making the power deposition independent of the number of slices actually acquired, hence the acronym PINS (power independent of number of slices). The power deposition per slice is hence dramatically reduced over conventional imaging techniques, thus making possible a new range of applications. The properties of these pulses will be explored, and some simple optimization performed to explore possible improvements to the slice profile at a fixed pulse duration.

THEORY

Pulse Design

The frequency spectrum of any known nonadiabatic RF pulse can be made periodic simply by multiplying its time domain envelope by a Dirac comb function (also known as a "picket fence" or "shah" function). This multiplication in the time domain is the equivalent of a convolution in the frequency domain. It is hence subjected to the same constraints as any other digitization process and therefore the sampling must at least fulfil the Nyquist condition with respect to the highest modulation frequency present in the RF envelope. More commonly, the sampling frequency will be determined by the ratio of the periodicity of the excitation to the slice thickness, which shall be denoted by N. For example, if a gaussian pulse has a slice thickness defined by its full width at half maximum bandwidth (BW), N is then given directly by the number of sampling periods of the Dirac comb that occur between the full width at half maximum values of the pulse in the time domain. To illustrate the PINS principle, Fig. 1 shows the standard approach to

[1]Radboud University Nijmegen, Donders Institute for Brain, Cognition and Behaviour, Donders Centre for Cognitive Neuroimaging, Nijmegen, The Netherlands.

[2]Erwin L. Hahn Institute for Magnetic Resonance Imaging, UNESCO-Weltkulturerbe Zollverein, Leitstand Kokerei Zollverein, Essen, Germany.

[3]MIRA Institute for Biomedical Technology and Technical Medicine, University of Twente, Enschede, The Netherlands.

*Correspondence to: Prof. Dr. David G. Norris, Ph.D., Donders Centre for Cognitive Neuroimaging, Trigon 240, Kapittelweg 29, NL-6525 EN, Nijmegen, The Netherlands. E-mail: David.Norris@donders.ru.nl

Received 1 July 2011; revised 21 July 2011; accepted 25 July 2011.

DOI 10.1002/mrm.23152

Published online 29 August 2011 in Wiley Online Library (wileyonlinelibrary.com).

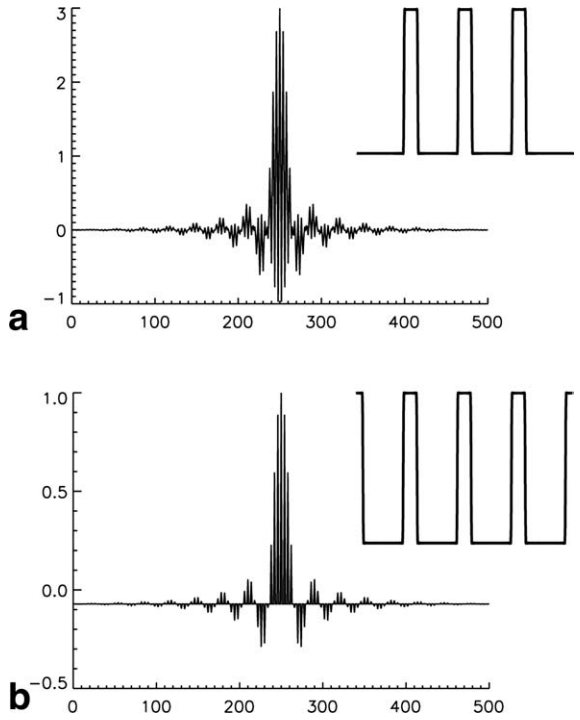

FIG. 1. **a:** A conventional multiplexed pulse to excite three slices. The basic pulse is a Hamming filtered sinc, and the profiles shown in the inset were obtained by Fourier transform. **b:** The same Hamming filtered sinc pulse multiplied by a Dirac comb function to excite slices with the same separation as in (a).

multiplexing using a Hamming filtered sinc pulse to excite three slices, and for comparison the PINS implementation of the same pulse to give an infinite series of slices having the same separation and profile as the conventional multiplexed pulse.

An alternative approach is to follow that of Hore (15) and to generate the RF pulse as a Fourier series expansion. Consider a periodic function $h(\omega)$, with period 2π, such that $h(\omega)$ has the value of unity in the range $-\pi/N \leq \omega \leq \pi/N$ and zero elsewhere within the period (this is consistent with the definition of N given in the previous paragraph). The Fourier expansion of $h(\omega)$ is then an even function given by

$$h(\omega) = \frac{1}{N} + \sum_{m=1}^{m=\infty} \frac{2}{\pi m} \sin\frac{m\pi}{N} \cos m\omega. \quad [1]$$

The time domain representation of Eq. 1 is

$$H(t) = \frac{1}{N}\delta(t) + \sum_{m=1}^{m=\infty} \frac{1}{\pi m} \sin\frac{m\pi}{N} \{\delta(m-t) + \delta(m+t)\}. \quad [2]$$

which is a sinc-modulated string of delta functions that will be truncated at $m = M$, where M is the number of terms in the Fourier expansion. Now in this description there is a time interval between the subpulses of unity, and the k-space traversed during this interval will define the mapping between frequency and space. The sinc modulation function will have its first zero at $m = N$, and hence for larger values of N, that correspond to the slice taking a smaller fraction of the period, the sinc function will be played out more slowly in time. The Fourier series expansion approach is equivalent to the multiplication of a sinc pulse by a truncated Dirac comb function. The number of lobes in the sinc is determined by the ratio of M to N. The value of $N = 2$, which corresponds to half of the period being excited, then has one nonzero delta function at the centre of each side lobe of the sinc and three at the central lobe. Lower values of N, which would lead to more than half the imaging volume being excited will not be considered here. Parenthetically, the Fourier series expansion approach can easily generate excitation patterns having a periodic variation in the phase.

Implementation

The approach advocated here for multiplexed imaging is to uniformly cover the volume of interest by performing N excitations, with the position of the periodically excited slices being manipulated by means of a phase gradient applied in the time domain. The minimum spatial periodicity of excitation that can be reconstructed without unacceptable levels of G-noise will be determined by the geometry of the receiver coil configuration and the efficiency of the partial parallel reconstruction technique. The ratio of this periodic length to the desired slice thickness will determine N, and the degree of truncation artifact that is acceptable together with the maximum acceptable pulse duration will determine M. Excitation pulses will require the application of a slice rephase gradient. The following implementation schemes may be considered:

(a) Application of the RF pulse train during a continuous gradient.
(b) Application of gradient pulses between the RF pulse subpulses.

These implementations were described previously (12) where it was noted that the application of a continuous gradient would lead to a further sinc modulation of the pulse angle over the imaged volume, and further that in implementation (a) the RF subpulse duration should be equal for all subpulses, whereas in implementation (b) power deposition could be further reduced by making the subpulse amplitudes equal but varying their durations. For the purpose of the current investigation, implementation (a) is considerably less attractive as it will result in an increase in power deposition compared to the non-PINS implementation of the same pulse, although the power per slice may still be reduced. Implementation (b) will give a power deposition equal to that of the non-PINS implementation in the limit of infinitesimal gradient pulse durations, which as will be demonstrated, will in practice lead to considerable reductions in the RF power deposition per slice. Another advantage of implementation (b) is that the flip angle should be uniform in space; however, if a compact pulse is desired with a high value of M, then the available gradient slew rate may become a limiting factor. Implementation (b) could be considered as the result of applying the VERSE technique to implementation (a) in the limit where the gradient is turned off during the RF pulse. Whichever of the two implementations is chosen, reversing the

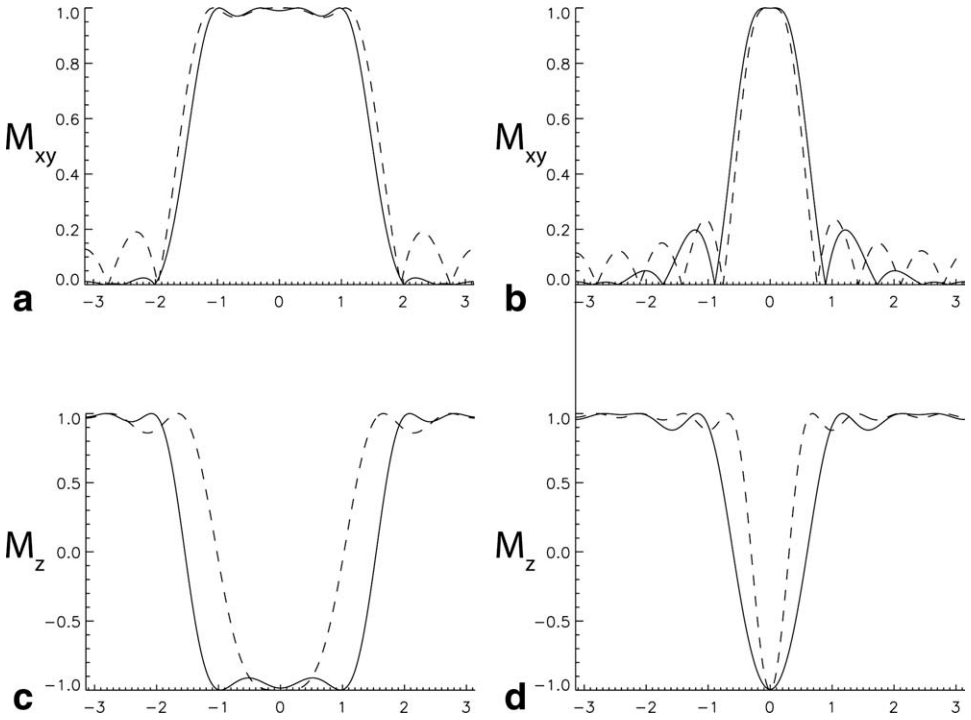

FIG. 2. Simulated RF pulse profiles for an RF pulse with $M = 4$, i.e., nine subpulses. The continuously drawn lines represent optimized profiles. The dashed lines show the profiles obtained using RF pulses obtained by Fourier expansion. The top row shows the transverse magnetization obtained for $N = 2$ (**a**) and $N = 8$ (**b**) for a 90° excitation pulse. The bottom row shows the profile of the longitudinal magnetization for an inversion pulse with $N = 2$ (**c**) and $N = 8$ (**d**).

polarity of the gradient will reverse the position of the chemical shift artefact, which can be used for fat suppression in a spin-echo sequence (16).

METHODS AND RESULTS

Simulation

Computer simulation was performed to calculate the slice rephase gradient strength and to explore the degree to which pulse performance could be optimized by varying the amplitude of the subpulses. Programs were written in IDL (ITT visual information solutions) and MATLAB (The Mathworks Inc., Natick, MA). For ease of simulation scheme (b) was used as the pulse train can then be represented as a series of rotations about the x' and z axes. For excitation pulses defined by Eq. 2, the refocusing gradient was found to be equal to M times the gradient area between the RF subpulses, independent of both M and N for flip angles up to 90°. This corresponds to the classical result for low flip angle excitation pulses, that the minimum rephase gradient is half the total gradient amplitude applied during the RF pulse.

Some simple simulations were also performed to explore the extent to which PINS pulse profiles could be optimized for low values of M. An iterative approach that varied the RF-subpulse amplitude while maintaining the symmetry of the pulse was used to account for the nonlinearity of the Bloch equations (17). The least squares difference was minimized between a target function having a value of 1 within the slice and 0 outside for transverse magnetisation in the optimization of excitation pulses, and −1 within the slice and 1 outside for longitudinal magnetization in the optimization of inversion/refocusing pulses. Simulations were conducted at $M = 4$, for $N = 2$ and $N = 8$. The resulting profiles are shown in Fig. 2, with the optimized profiles plotted with a continuous line and the original profiles shown for reference with a dashed line. The left plots (a and c) show the results for $N = 2$, the top plots (a and b) show the transverse magnetisation generated for a 90° pulse, and the bottom two the inversion profiles. The results clearly show that as the value of N increases (corresponding to thinner slices) the slice profile deteriorates, particularly for excitation. This is a fundamental property because thinner slices imply a reduction in pulse BW for the same pulse duration. The nonlinearity of the Bloch equations gives more scope for improving the 180° pulses because the nonlinearity has the effect of significantly reducing the BW of the nonoptimized pulse.

The PINS pulses were implemented in a simple spin-echo sequence, shown schematically in Fig. 3. Phantom and brain data were acquired on a 1.5 T Siemens Avanto and a 3 T Siemens Trio system, respectively, using a 32-channel head coil. Unless stated otherwise, a sagittal slice orientation was chosen in all experiments, so that the number of slices excited would be limited by the dimensions of the head. The gradient polarity was reversed between the excitation and refocusing pulses to eliminate the fat signal in the in vivo experiment (18). The general setup of the experiments consisted of acquiring a reference dataset using single slice sinc pulses with a matrix size of 32 × 32. These data were used to estimate the GRAPPA kernel to reconstruct the data of the multislice experiment in which four to five slices acquired on a matrix of 256 × 256 were collapsed into a single slice. The reconstruction method is described in detail in Ref. 19. It is important to note that in order for the reconstruction quality to be independent of off-resonance effects like chemical shift, the BW of the sinc pulses used to acquire the reference data was kept the same as the BW of the multislice pulses as defined in Eq. 2. To assess the quality of the reconstruction, we

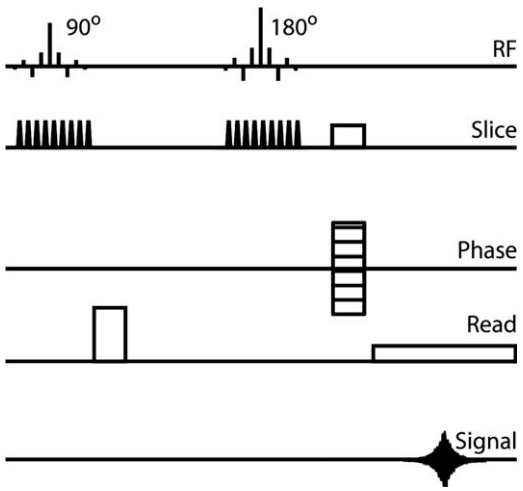

FIG. 3. Schematic pulse sequence of the spin-echo experiment. The PINS pulses are shown as sampled sincs, with each RF subpulse followed by a triangular gradient blip.

repeated the single slice reference scans with a 256 × 256 matrix to serve as a gold standard.

Figures 4 and 5 show the results of phantom experiments at 1.5 T. Scan parameters were: echo time = 50 ms, pulse repetition time = 525 ms, flip angle 90°, BW = 130 Hz/px. To be able to depict the slice profile, a relatively high inplane resolution of 1 × 1 mm^2 was used in combination with a slice thickness of 5 mm to retain signal-to-noise ratio (SNR). An image of the slice profile (Fig. 4) was obtained by placing a bottle in the middle of the headcoil and simply orienting the readout gradient along the slice axis, while holding all other parameters constant. Scan orientation was transversal in this case, i.e., slices perpendicular to the axis of the bottle, to maximize symmetry. The slice periodicity was 35 mm (i.e., $N = 7$, for a 5 mm slice), and the total duration of the RF pulses (both excitation and refocusing) was set to 5.12 ms. These parameters together with the slew rate allowed 21 RF subpulses to be transmitted, giving $M = 10$. Other relevant pulse parameters are RF subpulse duration 110 μs; gradient blip duration = 140 μs; maximum gradient amplitude 9.59 mT/m; blip gradient moment 0.67 ms mT/m. In a second phantom experiment on two bottles, the periodic slice profile excited and refocused five sagittal slices that were collapsed on top of each other. These were disentangled using a 7 × 8 GRAPPA kernel estimated from the 32 matrix reference data (8 × 8 × 5 mm^3). The reconstructed slices and their gold standard counterparts are shown in Fig. 5b and a, respectively. To illustrate the quality obtained, the difference between the two images is shown in Fig. 5c.

The experiment above was repeated at 3 T on a human volunteer after informed consent was given according to local ethics committee guidelines. The slice thickness was reduced to 4 mm, other changed parameters were pulse repetition time = 1050 ms, $M = 11$, $N = 10$, RF subpulse duration = 100 μs, gradient blip duration = 120 μs, maximum gradient amplitude = 9.79 mT/m, and pulse duration = 5.12 ms. The slice periodicity was increased to 40 mm, and a 4-fold acceleration factor was used. These results are shown in Fig. 6. Attempts to use more ambitious acceleration factors resulted in an unacceptable increase in G-noise at the centre of the brain. The difference image shown in Fig. 6c contains some unavoidable artifacts caused by motion but importantly no evidence of residual interference between slices. The frequency separation between fat and water at 3 T is 425 Hz, corresponding to a period of 2.35 ms, whereas the PINS pulse has 220 μs between each subpulse. So the shift of the fat slice is about one-tenth of the slice periodicity or approximately 4 mm. As the shift for the excitation and refocusing pulses is in opposite directions, the fat signal should be completely eliminated. The power deposited by the PINS pulses in this experiment is a factor of 2.2 higher than that for an equivalent non-PINS pulse; hence, the total power deposited for the acquisition of four slices of data is only 55% of that required for a conventional multislice imaging experiment.

DISCUSSION

A broad range of periodic pulses can be generated using the PINS procedure. The only major exception is that

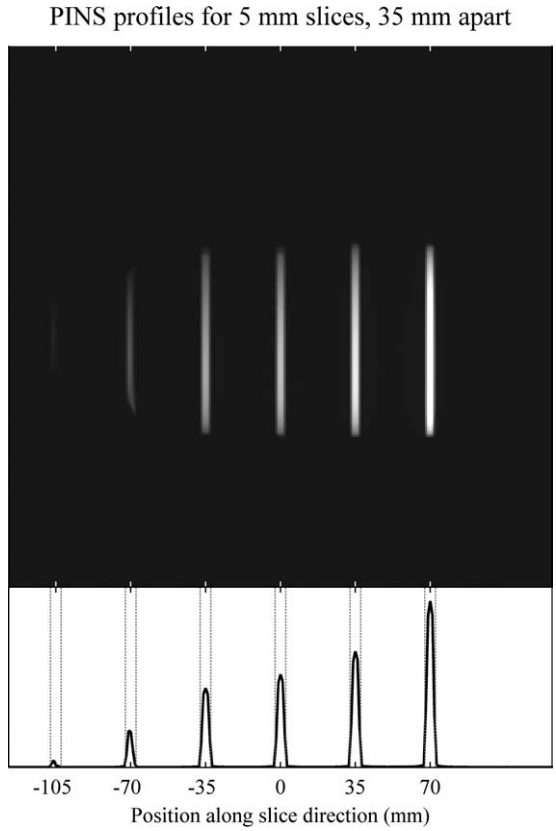

FIG. 4. An image (top) and its projection (bottom) of the slice profile of the PINS pulses that were used in the experiment shown in Fig. 5. Very sharp delineation of the slices can be observed without any residual signal (ringing) in between the slices. It should be noted that the profile results from the combined application of the excitation and refocusing pulses and does not attempt to show the profile for a single pulse. The variation in intensity is caused by RF inhomogeneities unrelated to the properties of the RF pulses; furthermore, the two slices on the left are outside the headcoil.

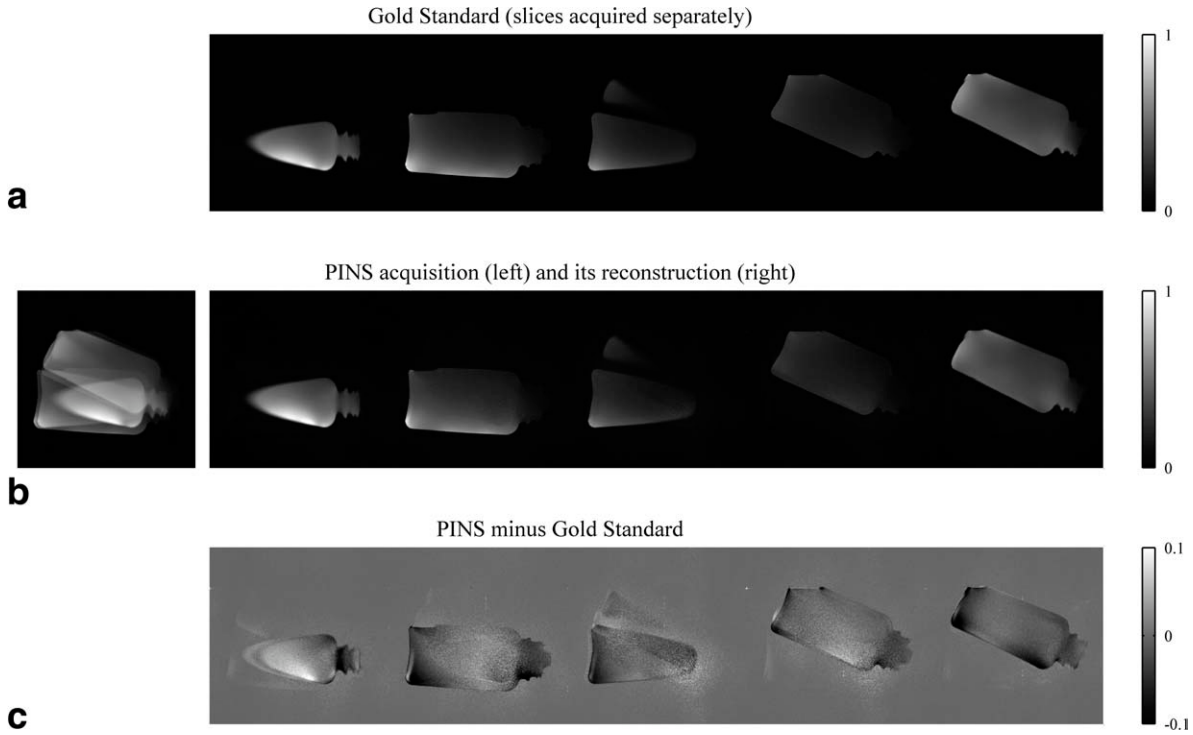

FIG. 5. Phantom experiment results of 5-fold PINS acceleration. As a gold standard reference, five individually scanned slices are shown in (**a**). Using PINS pulses, these slices were simultaneously excited and refocused resulting in a collapsed image (**b**; left panel). Using a 7 × 8 GRAPPA kernel, the collapsed image was disentangled yielding a result (b) almost identical to (a). The difference with respect to the gold standard image is shown in (**c**).

adiabatic pulses, such as the hyperbolic secant pulse (20), cannot be multiplexed in this way because it is not possible to satisfy the adiabatic condition for all resonance offsets. In the current application, the pulse duration is fairly long, which is determined to a great degree by the slow convergence of the sinc expansion. Hence, for some applications gaussian or similar pulses with a lower BW per unit time may be preferable. The duration of RF pulses should be considerably less than T_2^*, and in the presence of inhomogeneity gradients in the main magnetic field lengthy pulses may lead to distorted slice profiles. The time between the subpulses of the PINS pulse will determine the chemical shift artifact. In general, the longer duration of these pulses result in increased levels of chemical shift artifact in comparison to standard RF pulses. Dependent on the static magnetic field strength and the RF pulse parameters, additional presaturation of the fat resonance may be necessary, particularly for gradient echo sequences. For spin-echo sequences, and provided that a good static field homogeneity is realized, the gradient reversal technique used in this article (18) may be utilized. The fat signal will then be completely eliminated provided that the inequality $2\Delta t\Delta f N \geq 1$ is satisfied, where Δt is the interval between two consecutive subpulses in the RF pulse and Δf the chemical shift separation of fat and water in Hertz. If the RF amplitude is held constant and the duration between the subpulses varies, then the off-resonance behavior will be poorly defined leading to a smeared slice profile for off-resonance spins. Despite these caveats, this article demonstrates an excellent image quality both in phantoms and in vivo, as well as an excellent slice profile in phantom experiments. The acceleration factors obtained are comparable with those obtained with standard multiplexed RF pulses (7,8). Further improvements can be expected through the combination of PINS with the CAIPIRINHA method (21), which will either reduce the G-noise in the reconstruction or permit more slices per excitation at constant G-noise. This is a potentially significant improvement as the PINS approach is primarily limited by the maximum acceleration factor possible without unacceptable noise amplification. Furthermore, reducing the gap between slices not only further accelerates the acquisition but also reduces the value of N, leading to either shorter RF pulses or an improved profile at the same duration.

The number of slices excited is limited only by the physical dimensions of the object, the excitation volume of the transmit coil, and less critically the coverage of the gradient coil along the slice direction. This may necessitate the collection of larger amounts of reference data, and potentially increase the G-noise, particularly if the excitation coil excites a larger volume than the receiver array, leading to a number of excited slices that are primarily detected only by the receiver coils at the edge of the array, and with a potentially low SNR. If this problem is significant, then it may be solved by the additional application of spatially selective saturation pulses, but this solution will increase the RF power deposition. In many situations, the application of PINS pulses will require that the slice direction coincides with a circumscribed dimension of the object, e.g.,

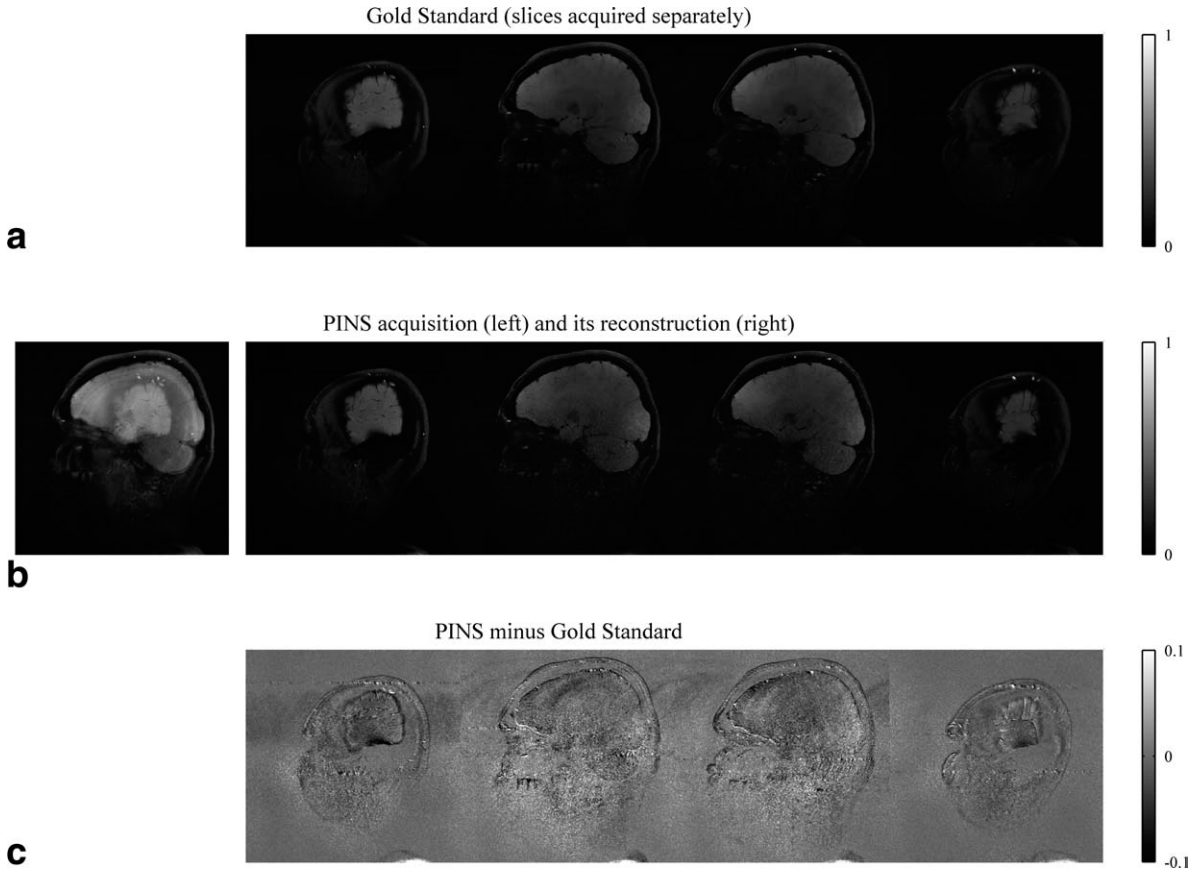

FIG. 6. In vivo results of 4-fold PINS acceleration obtained in sagittal section from the head of a healthy volunteer. Four individually scanned slices (**a**) serve as a gold standard reference to the PINS data in (**b**). A difference image is shown in (**c**). Enhanced noise levels can be seen in the middle of the brain. The ghosting artifacts seen in the first three slices are not due to the PINS approach but turned out to be present in the gold standard data. Edge effects are caused by motion between acquisitions which could not be corrected (through-slice motion). The difference image does not show hints of failed disentangling of the slices.

sagittal or coronal section in brain imaging, For spin-echo-based sequences, this restriction could be loosened by using conventional multiplexing techniques to generate the 90° pulses and PINS for the more power intensive refocusing pulses. The ability to excite large numbers of slices can, however, be turned as an advantage in many situations as it will enable the scanning of considerable volumes of tissue within a short duration, provided that an adequate number of receiver coils can be used.

The most commonly used technique for reducing RF power deposition is VERSE (22), which can achieve reductions of up to a factor of about four. The greatest reductions with VERSE can be attained for pulses with a high BW-time product, whereas PINS will primarily use low BW pulses. Nevertheless, the two approaches are not mutually incompatible, as both approaches described in the Implementation section could benefit from the application of VERSE.

This article has concentrated on the properties of the PINS RF pulses and has not explored the range of pulse sequences with which they can be combined. In principle, all conventional two-dimensional sequences could benefit from this approach, with the greatest gains being obtained for those sequences that have intrinsically high power deposition, particularly at high main magnetic field strengths. Particular gains can hence be expected for rapid acquisition with relaxation enhancement (RARE)/fast spin-echo (FSE) type sequences, and at very high field strengths, such as 7 T spin-echo echo-planar imaging and diffusion-weighted echo-planar imaging will benefit. In echo-planar imaging, the conventional CAIPIRINHA method could be replaced by the recently developed blipped CAIPIRINHA technique (23), and further acceleration of the acquisition may be obtained by incorporating the simultaneous echo refocusing (SIR) technique (24). Furthermore, the ability to potentially manipulate the phase of a periodic subset of slices offers the potential to further accelerate the acquisition in a wide range of application sequences by using the XUN-FOLD technique (25).

Ultimately, the decoupling of the RF power deposition from the number of slices being acquired could lead to a redesign of scanner hardware and sequence implementation so that whole organ or indeed whole body data are acquired within a fraction of the duration currently required.

In conclusion, the RF pulses described here, when combined with multiplexed parallel imaging (6), open up new perspectives for the rapid imaging of large volumes of tissue; whole body imaging and spin-echo-based sequences at high static magnetic field strengths.

ACKNOWLEDGMENTS

D.G. Norris and P.J. Koopmans contributed equally to this work.

REFERENCES

1. Bolinger L, Leigh JS. Hadamard spectroscopic imaging (HSI) for multivolume localization. J Magn Reson 1988;80:162–167.
2. Glover GH. Phase-offset multiplanar (POMP) volume imaging—a new technique. J Magn Reson Imaging 1991;1:457–461.
3. Sodickson DK, Manning WJ. Simultaneous acquisition of spatial harmonics (SMASH): fast imaging with radiofrequency coil arrays. Magn Reson Med 1997;38:591–603.
4. Prüssmann KP, Weiger M, Scheidegger MB, Bösiger P. SENSE: sensitivity encoding for fast MRI. Magn Reson Med 1999;42:952–962.
5. Griswold MA, Jakob PM, Heidemann RM, Nittka M, Jellus V, Wang J, Kiefer B, Haase A. Generalized autocalibrating partially parallel acquisitions (GRAPPA). Magn Reson Med 2002;47:1202–1210.
6. Larkman DJ, Hajnal JV, Herlihy AH, Coutts GA, Young IR, Ehnholm G. Use of multicoil arrays for separation of signal from multiple slices simultaneously excited. J Magn Reson Imaging 2001;13:313–317.
7. Moeller S, Yacoub E, Olman CA, Auerbach E, Strupp J, Harel N, Ugurbil K. Multiband multislice GE-EPI at 7 Tesla, with 16-fold acceleration using partial parallel imaging with application to high spatial and temporal whole-brain FMRI. Magn Reson Med 2010;63:1144–1153.
8. Feinberg DA, Moeller S, Smith SM, Auerbach E, Ramanna S, Glasser MF, Miller KL, Ugurbil K, Yacoub E. Multiplexed echo planar imaging for sub-second whole brain FMRI and fast diffusion imaging. PLoS ONE 2010;5:e15710.
9. Zerhouni EA, Parish DM, Rogers WJ, Yang A, Shapiro EP. Human-heart—tagging with MR imaging—a method for noninvasive assessment of myocardial motion. Radiology 1988;169:59–63.
10. Axel L, Dougherty L. MR imaging of motion with spatial modulation of magnetization. Radiology 1989;171:841–845.
11. Axel L, Dougherty L. Heart wall motion: improved method of spatial modulation of magnetization for MR imaging. Radiology 1989;172:349–350.
12. Wu EX, Towe CW, Tang HY. MRI cardiac tagging using a sinc-modulated RF pulse train. Magn Reson Med 2002;48:389–393.
13. Pope JM, Yao S. Flow-selective pulse sequences. Magn Reson Imaging 1993;11:585–591.
14. Norris DG, Schwarzbauer C. Velocity selective radiofrequency pulse trains. J Magn Reson 1999;137:231–236.
15. Hore PJ. Solvent suppression in Fourier transform nuclear magnetic resonance. J Magn Reson 1983;55:283–300.
16. Gomori JM, Grossman RI, Yu-Ip C, Asakura T. NMR relaxation times of blood: dependence on field strength, oxidation state, and cell integrity. J Comput Assist Tomogr 1987;11:684–690.
17. Lurie DJ. A systematic design procedure for selective pulses in NMR imaging. Magn Reson Imaging 1985;3:235–243.
18. Gomori JM, Holland GA, Grossman RI, Gefter WB, Lenkinski RE. Fat suppression by section-select gradient reversal on spin-echo MR imaging. Radiology 1988;168:493–495.
19. Blaimer M, Breuer FA, Seiberlich N, Mueller MF, Heidemann RM, Jellus V, Wiggins G, Wald LL, Griswold MA, Jakob PM. Accelerated volumetric MRI with a SENSE/GRAPPA combination. J Magn Reson Imaging 2006;24:444–450.
20. Silver MS, Joseph RI, Hoult DI. Highly selective 90° and 180° pulse generation. J Magn Reson 1984;59:347–351.
21. Breuer FA, Blaimer M, Heidemann RM, Mueller MF, Griswold MA, Jakob PM. Controlled aliasing in parallel imaging results in higher acceleration (CAIPIRINHA) for multi-slice imaging. Magn Reson Med 2005;53:684–691.
22. Conolly S, Nishimura D, Macovski A. Sweep-diagram analysis of selective adiabatic pulses. J Magn Reson 1989;83:549–564.
23. Setsompop K, Gagoski B, Polimeni JR, Witzel T, Wedeen V, Wald LL. Blipped-CAIPIRINHA for simultaneous multi-slice EPI with reduced g-factor penalty. Magn Reson Med; in press.
24. Feinberg DA, Reese TG, Wedeen VJ. Simultaneous echo refocusing in EPI. Magn Reson Med 2002;48:1–5.
25. Stenger VA, Giurgi MS, Boada FE, Noll DC. Excitation UNFOLD (XUNFOLD) to improve the temporal resolution of multishot tailored RF pulses. Magn Reson Med 2006;56:692–697.